Bull. Mater. Sci. (2020) 43:65
https://doi.org/10.1007/s12034-019-2023-x

Few-layer-graphene as intercalating agent for spray-pyrolysed fluorine-doped tin oxide transparent conducting electrode

L GO, L MACARAIG and E ENRIQUEZ*
Department of Chemistry, Ateneo de Manila University, Katipunan Ave., Loyola Heights, Quezon City 1108, Philippines
*Author for correspondence (epenriquez@ateneo.edu)

MS received 8 July 2019; accepted 19 September 2019

Abstract. In this work, the development of a robust method for the fabrication of a low-cost transparent conducting electrode (TCE) *via* the addition of graphene in the spray-pyrolysis of fluorine-doped tin oxide (FTO) is explained. Alcoholic suspensions of few-layer-graphene were produced *via* the liquid exfoliation of graphite in different alcoholic solutions as sonicating solvent. These mixtures were then mixed with ammonium fluoride and tin (II) chloride dihydrate precursors to fabricate graphene/FTO composite through spray pyrolysis. Graphene exfoliated with 50% aqueous ethanol proved to yield improved TCE properties with nearly two-fold enhancement in figure of merit (FOM) measured in terms of the ratio of optical transmittance and sheet resistance. Using optimized spraying conditions, graphene/FTO coatings still yielded slightly higher FOM compared to plain FTO. The increase in FOM is largely attributed to the decrease in sheet resistance with the incorporation of graphene flakes.

Keywords. Transparent conducting electrode; few-layer-graphene; spray pyrolysis.

1. Introduction

Transparent conducting electrodes (TCEs) made from doped metal oxide semiconductors are already widely known and widely used in optoelectronics and photovoltaic applications. Metal oxides themselves are semiconducting, but when positively or negatively doped, can become highly conducting. Two doped metal oxides are primarily used, indium tin oxide (ITO) [1–3] and fluorine-doped tin oxide (FTO) [4,5]. Despite its higher conductivity, ITO has lower stability at high temperatures and therefore, cannot be used for devices that need to be heated at high temperatures (>400°C) during fabrication [6]. For example, FTO is more commonly used in devices like perovskite [7] or dye-sensitized [8,9] solar cells that have a TiO_2 layer deposited on FTO and post-annealed in air at high temperatures to form the anatase phase. Also, ITO electrodes are more expensive than FTO, since indium is a rare earth metal and its high demand has increased its price significantly [10]. With increasing usage in optoelectronic devices, there is need for a cheaper and more conductive alternative. Graphene, after its discovery in 2004 by Novoselov *et al* [11], has been the centre of research for TCEs in optoelectronic devices. With an intrinsic high electrical sheet conductivity [12] and high optical transparency [13], there are various works on the use of graphene as TCE. Another major advantage of graphene is its high abundance compared with other doped-metal oxide electrodes. Successful fabrication of large area graphene using chemical vapour deposition (CVD) has been reported [14]. This process, though promising, needs expensive equipment and starting materials, thus, alternative method such as the deposition of liquid exfoliated graphene flakes gained popularity. However, the latter method has not had as much success due to low interparticle connectivity between the flakes when they are deposited [15]. Graphene flakes prepared *via* solution method produces a sheet resistance ∼1500 Ω/□, too high for optoelectronics or solar cell use [16]. Nonetheless, multilayer or few-layer-graphene (FLG) derived through liquid exfoliation remains to be a suitable candidate for large-volume applications [17].

Like graphene, the more inexpensive metal oxide TCE alternative, FTO is produced *via* physical vapour deposition (PVD) and CVD, with the CVD pyrolysis furnace still the most commonly implemented instrument for film deposition [18]. A cheaper process *via* spray-pyrolysis deposition (SPD) can significantly reduce the cost of production and it also produces FTO films with good transparency and acceptable electrical properties [19–21]. However, the turbulence effect of spray on the boundaries of the substrate make it difficult to produce films with excellent uniformity. Large-area rainbow patterns are apparent in most films. These non-uniformities were attributed to the non-uniform and varying ratios of the fluorine dopant to tin oxide [18] across the film.

In this work, a method was developed wherein graphene flakes that have been exfoliated from graphite powder are incorporated into the FTO precursor solutions, this in turn was used to form a composite which is expected to improve the conductivity of FTO TCEs prepared *via* SPD. In essence, this approach to form the composite compensates for the negative effect of turbulent spray which usually results in lower

Published online: 10 February 2020

conductivity. Typically, tin oxide is prepared *via* SPD either from tin (II) chloride ($SnCl_2$) [22] or tin (II) chloride dihydrate ($SnCl_2{\cdot}2H_2O$) [23] or tin (IV) chloride ($SnCl_4$) [24] or tin (IV) chloride pentahydrate ($SnCl_4{\cdot}5H_2O$) [25]. The fluorine dopant can either be ammonium fluoride (NH_4F) [26] or hydrofluoric acid [24]. In this work, $SnCl_2{\cdot}2H_2O$ was used as the tin source as it is cheaper than $SnCl_4$; whereas NH_4F was used as the fluorine source because of its lower hazard risk. The SPD was done in a straightforward spray pyrolysis setup, which used readily available laboratory paraphernalia.

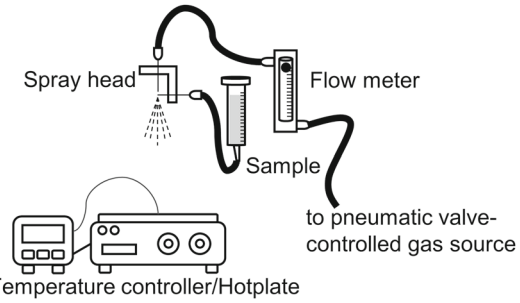

Figure 1. Diagram of the spray pyrolysis setup used.

2. Methodology

2.1 *Alcohol solutions for graphene exfoliation*

Three different concentrations of alcohols were used for the liquid exfoliation of graphene: 50% aqueous ethanol (v/v), 70% aqueous isopropanol and 50% ethanol–isopropanol. The exfoliation was done by adding 0.5 g of graphite powder (Ansac Sendirian Berhad) to 100 ml of the alcohol solutions followed by ultrasonic treatment for 1.5 h in an ultrasonic bath (Cole-Palmer 8852 bath sonicator, 352 Watts output). The graphene suspensions were then centrifuged (Thermo, Sorvall Legend RT) at 4500 rpm for 1.5 h to remove large unexfoliated graphite particles.

2.2 *Graphene/NH_4F doping of $SnCl_2$*

The concentrations of the tin and fluorine precursors were adopted from the work of Miao *et al* [27], but instead of using pure ethanol solvent, alcoholic graphene suspensions were used. The different alcohol systems were tested with a low amount of fluorine doping (0.7 wt%). All subsequent runs used a fluorine dopant concentration of 10 wt%, since several studies have found that the sheet resistance of FTO significantly decreases as fluorine doping concentration increases to 10 wt%; adding more fluorine only changes the sheet resistance minimally [14,27,28]. Experimentally, 11 g of $SnCl_2{\cdot}2H_2O$ (JT Baker) and 1.1 g of NH_4F (JT Baker) were dissolved in 100 ml of graphene stock solutions. The solution was then stirred for 10 min. While stirring, 1 ml of HCl was added to increase the pH of the solution and to clear out the turbidity due to insoluble tin hydroxide precipitated from the reaction of $SnCl_2$ and water. The remaining precipitates and larger FLG flakes were then removed by centrifugation at 4500 rpm for 2 min.

2.3 *Spray pyrolysis*

Freshly prepared precursor solutions were spray-pyrolysed using needle nozzles for precursor inlet and carrier gas inlet at 90°. This was mounted on a stand with the spray head above a piranha solution-cleaned glass substrate (Corning microscope slide cut into 25 × 25 mm^2). The glass substrate was placed on top of a hot plate and heated at 400°C with the hot plate controlled by a digital controller (West instrument model N2300 Y1210S140). Nitrogen gas was used as the carrier gas, which was electronically switched on and off using an electrically controlled pneumatic valve (Airtac model 4V210-08), while being monitored by a pressure gauge (standard pressure gauge with 0-60 PSI reading) and flow meter (Key instrument flow meter 0-30 LPM). The precursor solution was drawn from a conical vial with a tube connected to the solution inlet of the needle nozzle. The level of the solution was adjusted such that it is in the same level with the needle nozzle to eliminate the effect of hydrostatic pressure (figure 1). Different spray parameters, such as the nozzle-to-substrate distance, nitrogen gas pressure and flow rate, and the manner of spray bursts were initially optimized. The optimized setup was as follows: nozzle-to-substrate distance at 200 cm, the nitrogen gas sprayed at a pressure of 50 PSI and flow rate of 9 LPM, and a spray burst of 5 s, each allowing the substrate temperature to heat to the programmed temperature before the next burst is done. At least three slides were prepared per test precursor solution tested.

2.4 *Characterization*

The optical transparency against air of the TCEs was measured between 400 and 800 nm using a UV–visible spectrometer with an integrating sphere attachment (Shimadzu UV-2401 with ISR2200). The sheet resistance was measured by averaging the five measurements done using a Jandel four-point probe (tungsten carbide, 45 g loading, 40 mils probe distance; the outer two probes supplied constant current, while the inner two probes measured voltage). The thickness of the samples was measured using a surface profiler (KLA Tencor AlphaStep D600). Representative samples of the optimized films were characterized for crystal structure using an X-ray diffraction machine (XRD, Rigaku Ultima IV) at angle ranging from 20 to 80°, surface morphology using a scanning electron microscope (SEM, Hitachi SU1510), carrier mobility using a Hall effect apparatus (Ecopia HMS-3000) and Raman spectroscopy (Horiba Xplora Plus).

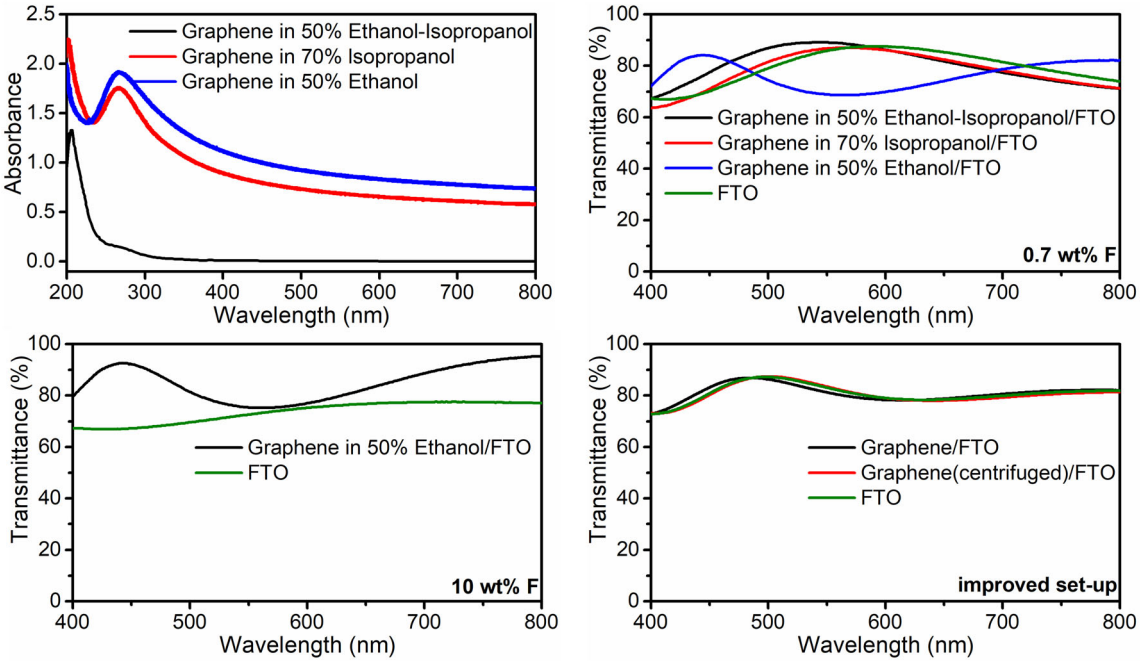

Figure 2. UV–Vis spectra of graphene suspension exfoliated using different alcohol systems and % transmittance data of the spray-pyrolysed electrodes against air.

3. Results

3.1 *Effect of alcohol type and concentration*

Graphene suspensions exfoliated using three different alcoholic-aqueous systems were characterized *via* UV–Vis spectroscopy (figure 2). The use of a 50% aqueous ethanol system shows to have more graphene in suspension, as indicated by the characteristic absorbance at 270 nm [29]. The baseline absorbance is also higher for the 50% aqueous ethanol system which is attributed to light scattering caused by suspended FLG. Figure 1 also shows that the 70% aqueous isopropanol mixture yielded a good amount of exfoliated graphene in suspension, whereas the 50% ethanol–isopropanol did not yield a good amount of graphene in suspension. The alcohol in the alcohol:water system helped in the dispersion of graphene given its non-polar property and yet nearly matching the required surface tension and net dielectric solvent property to stabilize the graphene suspension [30].

NH_4-doped $SnCl_2$ precursors were then added to the graphene suspensions, stirred for 10 min, centrifuged and then spray-pyrolysed. Three trials were done for each system as well as for the four-point probe readings (current and voltage). As a control, a FTO TCE without any graphene was also spray-pyrolysed using 70% aqueous isopropanol solvent. The sheet resistance of the graphene/FTO composite acquired from 50% aqueous ethanol had the best sheet resistance among all the TCEs (315 Ω/□). This is followed by the sheet resistance of graphene/FTO composite prepared from 70% aqueous isopropanol suspensions (439 Ω/□), which still has a better sheet resistance compared to plain FTO coating (491 Ω/□). The graphene/FTO coating prepared from 50% ethanol–isopropanol suspensions, however, showed poorer sheet resistance (590 Ω/□) compared to plain FTO coating (summarized in table 1). It was also noted during the experiment that the NH_4F did not dissolve very well in the pure alcohol system, which could have lowered the fluorine doping concentration and thus, increase the sheet resistance of the coating. Figure 1 shows that there is a correlation with the concentration of graphene in the spray mixture and the sheet resistance, where the sheet resistance decreases with the increasing graphene concentration in the spray suspension.

Since the intended application of the composite is for TCEs, the optical transparency was also measured. The average % transmittance was measured over the visible range of 400–800 nm against air (table 1). Figure 2 shows the corresponding transmission spectra, which are wavy due to the interference fringe pattern created by the thin-film coating. The % transmittance of the graphene/FTO coating prepared from 50% ethanol–isopropanol is the highest because of the low graphene loading and the graphene/FTO coating prepared from 50% aqueous ethanol suspensions is the lowest due to the relatively higher loading of graphene flakes in the former suspension.

The Hacke's figure of merit (FOM) was also computed using the following equation (1) (table 1) [30]. Hacke's FOM considers both sheet resistance (R_S) and optical transmittance (T) of a TCE and puts it into one value (equation 1).

Table 1. Sheet resistance, % transmittance and FOM of the different electrodes prepared from graphene/FTO precursors (standard deviation values are given in parentheses).

Electrode	Sheet resistance (Ω/□)	Transmittance (%)	FOM
Graphene in 50% ethanol–isopropanol/FTO (0.7 wt% F)	590 (39)	80.3 (0.5)	1.89×10^{-4}
Graphene in 70% isopropanol/FTO (0.7 wt% F)	439 (15)	78.5 (0.5)	2.02×10^{-4}
Graphene in 50% ethanol/FTO (0.7 wt% F)	315 (22)	76.3 (0.5)	2.13×10^{-4}
FTO (0.7 wt% F)	491 (6)	79.7 (0.5)	2.09×10^{-4}
Graphene in 50% ethanol/FTO (10 wt% F)	52 (6)	73.5 (0.5)	1.67×10^{-3}
FTO (10 wt% F)	118 (23)	85.0 (0.5)	8.85×10^{-4}

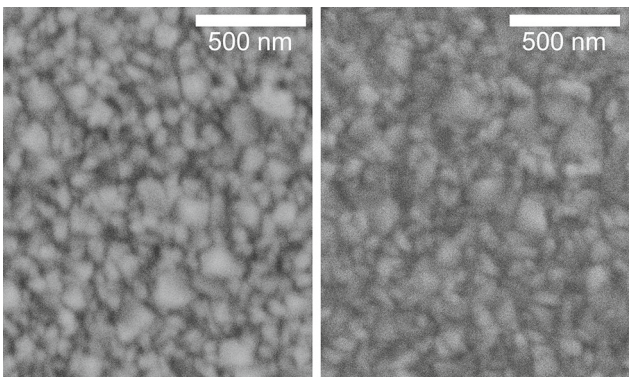

Figure 3. SEM micrographs of FTO (left) and graphene/FTO (right) films with the improved setup.

$$\text{FOM} = \frac{T^{10}}{R_S} \tag{1}$$

A high optical transmittance and low sheet resistance, or a higher value for the FOM is desirable for TCEs. The FOM is the highest for the coating from the 50% ethanol/FTO suspension.

3.2 *Increasing fluorine doping concentration to 10 wt%*

Since it was observed that the results were best with 50% aqueous ethanol as the exfoliating solvent, FTO–graphene composites were prepared using a fluorine doping concentration of 10 wt%, the optimum reported concentration for the F-dopant [27]. The sheet resistance of the resulting graphene/FTO coating decreased significantly to 52.4 Ω/□ compared to that of plain FTO, which also decreased to 118.4 Ω/□. Notably, the optical transparency of the graphene/FTO coating (85%) was also better than the optical transparency of the plain FTO (73.5%) (table 1, figure 2). The optical transparency of plain FTO with increased doping concentration (from 0.7 to 10%) decreased. This may be due to the decrease in the number of oxygen vacancies [31]. This decrease in sheet resistance for the graphene/FTO coating and the increase in transparency led to a significant

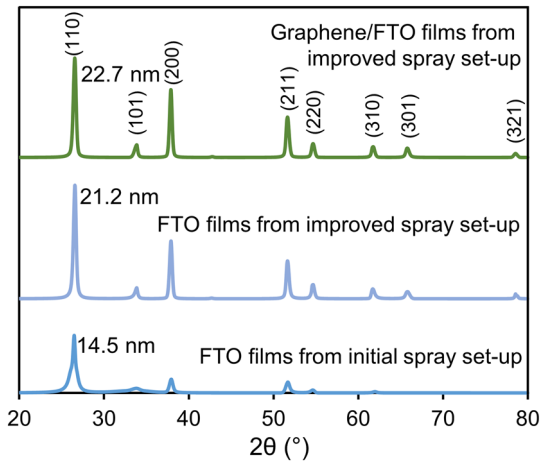

Figure 4. XRD pattern of FTO and graphene/FTO films with the initial and improved setups.

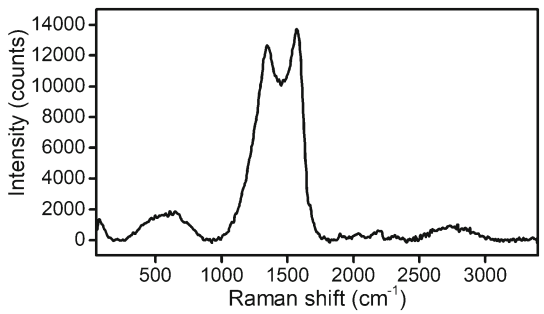

Figure 5. Raman spectra of graphene/FTO film with the improved setup.

increase, by one order of magnitude, in the FOM of the graphene/FTO coating compared to plain FTO (summarized in table 1).

3.3 *Removing large FLG flakes from precursor solution*

The spray setup was further improved by replacing the needle nozzle with an external mix single action airbrush. The airbrush allowed for a more controlled mist to reduce the abrupt

Table 2. Sheet resistance, % transmittance, FOM and electrical properties of the different electrodes prepared from graphene/FTO precursors with improved spray pyrolysis settings (standard deviation values are given in parentheses).

Electrode	Sheet resistance (Ω/□)	Transmittance (%)	FOM	Hall mobility ($cm^2V^{-1}s^{-1}$)	Resistivity (Ω cm)	Carrier concentration (cm^{-3})
FTO	22.2 (0.5)	80.4 (0.5)	5.08×10^{-3}	27	3.0×10^{-4}	1×10^{20}
Graphene/FTO	22.4 (0.2)	80.5 (0.5)	5.10×10^{-3}	27	3.0×10^{-4}	1×10^{20}
Graphene (centrifuged)/FTO	18.6 (0.5)	79.9 (0.5)	5.70×10^{-3}	28	2.9×10^{-4}	1×10^{20}

decrease in the temperature of the substrate. The decrease in substrate temperature affects the volatilization of fluoride as the spray drop approaches the substrate and the tin oxide crystallizes [18]. SEM images for FTO and graphene/FTO coatings show crack-free and relatively homogeneous films (figure 3). Peak intensities in the XRD pattern increased as the setup was changed from that of the initial setup (figure 4). The increase in crystallinity also manifested in the increase in the crystallite size beside the (110) peaks as indicated in figure 3 (as estimated by Scherrer's equation), is due to the better control of the substrate temperature, and the thickness of the SPD samples was nearly constant at ∼550 nm across the film. The graphene/FTO films showed a very slight improvement in crystallinity from the FTO films with the improved setup. This may be due to the small increase in actual film temperature due to the better thermal conduction of graphene, since higher substrate temperatures have shown to produce larger grains, higher crystallinity and lower surface roughness [32]. Also, the graphene/FTO films do not have a noticeable characteristic broad peak of graphene near 25° since the sharp (110) peak of FTO is in the same region. The presence of graphene is confirmed *via* Raman spectroscopy as shown in figure 5, which shows a pattern indicative of FLG [33].

The finer mist of the improved setup allowed for more evenly coated and doped films. This is noticeable in the standard deviation (SD) of the sheet resistance of the film using the nozzle compared with those using the airbrush (tables 1 and 2). With the improved setup, the FOM improved for both FTO and graphene/FTO coatings largely due to the lower sheet resistance. The average sheet resistance for plain FTO and graphene/FTO coatings is 22.2 (SD 0.5) Ω/□ and 22.4 (SD 0.2) Ω/□, respectively. To further decrease the sheet resistance, the centrifuge speed was increased to 12,000 rpm prior to spray pyrolysis to remove large FLG flakes. The resulting coating has a sheet resistance of 18.6 (SD 0.2) Ω/□. Since the % transmittance for plain FTO, graphene/FTO and graphene (centrifuged)/FTO are similar at 80% (table 2, figure 2), the FOM is the highest for the coating prepared from graphene/FTO precursors with large FLG flakes removed by centrifugation. A sample slide with graphene/FTO coating is pictured in figure 6. The electrical properties of the slides prepared from the improved setup were similar (table 2). These sheet resistance values make

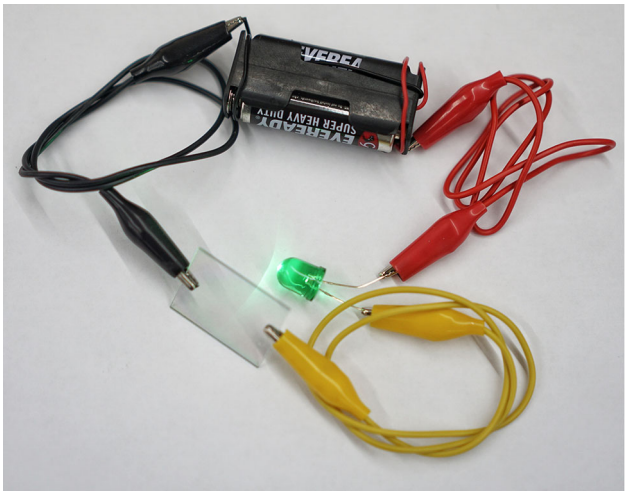

Figure 6. Demonstration of graphene/FTO-coated glass slide used as conductor to light an LED.

the FTO and graphene/FTO films useful as photoanodes for photovoltaic application [34].

4. Conclusions

The incorporation of graphene as intercalating agent in the precursor solution of FTO for SPD has made the deposition process more robust. Graphene/FTO composite coatings fabricated *via* spray-pyrolysis using a setup built from locally available materials, were shown to have lower sheet resistance, comparable transmittance and higher FOM when compared to FTO coatings without graphene. With graphene incorporation, the FOM increased by one order of magnitude even for FTO films that had non-uniformities due to non-ideal spray conditions. This increase in FOM is largely attributed to the decrease in sheet resistance for films with graphene.

Acknowledgements

The authors would like to thank the funding support of PCIEERDDOST, CHED-PCARI (IIID58) and the University Research Council of the Ateneo de Manila University.

EPE also thanks the Chevron Philippines, Inc. Endowed Professorial Chair.

References

[1] Ishibashi S, Higuchi Y, Ota Y and Nakamura K 1990 *J. Vac. Sci. Technol.* **8** 1403
[2] Latz R, Michael K and Scherer M 1991 *Jpn. J. Appl. Phys.* **30** 2A
[3] Hoertz P G, Chen Z, Kent C A and Meyer T J 2010 *Inorg. Chem.* **49** 8179
[4] Baek W H, Choi M, Yoon T S, Lee H H and Kim Y S 2010 *Appl. Phys. Lett.* **96** 133506
[5] Kim H, Auyeung R C Y and Piqué A 2008 *Thin Solid Films* **516** 5052
[6] Kawashima T, Matsui H and Tanabe N 2003 *Thin Solid Films* **445** 241
[7] Yang T-Y, Jeon N J, Shin H-W, Shin S S, Kim Y Y and Seo J 2019 *Adv. Sci.* **6** 1900528
[8] Koide N and Han L 2004 *Rev. Sci. Instrum.* **75** 2828
[9] San Esteban A C M and Enriquez E P 2013 *Sol. Energy* **98** 392
[10] Jansseune T 2005 *Compd. Semicond.* **11** 34
[11] Novoselov K S, Geim A K, Morozov S V, Jiang D, Zhang Y, Dubonos S V *et al* 2004 *Science* **306** 666
[12] Chen J-H, Jang C, Xiao S, Ishigami M and Fuhrer M S 2008 *Nat. Nanotechnol.* **3** 206
[13] Bae S, Kim H, Lee Y, Xu X, Park J-S, Zheng Y *et al* 2010 *Nat. Nanotechnol.* **5** 574
[14] Thangaraju B 2002 *Thin Solid Films* **402** 71
[15] De S and Coleman J N 2010 *ACS Nano.* **4** 2713
[16] Wang F J and Lin T C 2012 *Method for preparing graphene powder and graphene transparent conductive film by oxyhydrogen flame method*, CN103213970A
[17] Ramanathan T, Abdala A A, Stankovich S, Dikin D A, Herrera-Alonso M, Piner R D *et al* 2008 *Nat. Nanotechnol.* **3** 327
[18] Zhao X, Deng Y and Cheng J 2016 *Int. J. Electrochem. Sci.* **11** 5395
[19] Elangovan E and Ramamurthi K 2005 *Thin Solid Films* **476** 231
[20] Rakhshani A E, Makdisi Y and Ramazaniyan H A 1998 *J. Appl. Phys.* **83** 1049
[21] Subba Ramaiah K and Sundara Raja V 2006 *Appl. Surf. Sci.* **253** 1451
[22] Kulaszewicz S, Lasocka I and Michalski C 1978 *Thin Solid Films* **55** 283
[23] Jordan J F and Albright S P 1988 *Sol. Cells* **23** 107
[24] Grosse P, Schmitte F J, Frank G and Köstlin H 1982 *Thin Solid Films* **90** 309
[25] Fantini M and Torriani I 1986 *Thin Solid Films* **138** 255
[26] Kim H and Laitinen H A 1975 *J. Am. Ceram. Soc.*, https://doi.org/10.1111/j.1151-2916.1975.tb18974.x
[27] Miao D, Zhao Q, Wu S, Wang Z, Zhang X and Zhao X 2010 *J. Non-Cryst. Solids* **356** 2557
[28] Tuyen Le T, Jian S-R, Tien T N and Le H P 2019 *Materials (Basel)* **12** 1665
[29] Li D, Müller M B, Gilje S, Kaner R B and Wallace G G 2008 *Nat. Nanotechnol.* **3** 101
[30] Hernandez Y, Nicolosi V, Lotya M, Blighe F M, Sun Z, De S *et al* 2008 *Nat. Nanotechnol.* **3** 563
[31] Banyamin Z, Kelly P, West G and Boardman J 2014 *Coatings* **4** 732
[32] Tatar D, Turgut G and Düzgün B 2013 *Rom. J. Phys.* **58** 143
[33] Johra F T, Lee J-W and Jung W-G 2014 *J. Ind. Eng. Chem.* **20** 2883
[34] Fortunato E, Ginley D, Hosono H and Paine D C 2007 *MRS Bull.* **32** 242